Molecular Neurobiology

ISSN0893-7648/02/26(2–3): 235–250/$20.00

Structure of the Sodium Channel Gene *SCN11A*

Evidence for Intron-to-Exon Conversion Model and Implications for Gene Evolution

Sulayman D. Dib-Hajj,[1,2,3], Lynda Tyrrell,[1,2,3] and Stephen G. Waxman[*,1,2,3]

[1]Department of Neurology and [2]PVA/EPVA Neuroscience Research Center, Yale University School of Medicine, New Haven, CT 06510; and [3]Rehabilitation Research Center, Veterans Affairs Medical Center, West Haven, CT 06516

Abstract

Exon/intron boundaries in the regions encoding the trans-membrane segments of voltage-gated Na channel genes are conserved, supporting their proposed evolution from a single domain channel, while the exons encoding the cytoplasmic loops are less conserved with their evolutionary heritage being less defined. *SCN11A* encodes the tetrodotoxin-resistant (TTX-R) sodium channel Na_v 1.9a/NaN, which is preferentially expressed in nociceptive primary sensory neurons of dorsal root ganglia (DRG) and trigeminal ganglia. *SCN11A* is localized to human chromosome 3 (3p21–24) close to the other TTX-R sodium channel genes *SCN5A* and *SCN10A*. An alternative transcript, Na_v1.9b, has been detected in rat DRG and trigeminal ganglion. Na_v1.9b is predicted to produce a truncated protein due to a frame-shift, which is introduced by the new sequence of exon 23c (E23c). In human and mouse *SCN11A*, divergent splicing signals prevent utilization of E23c. Unlike exons 5A/N in genes encoding TTX-sensitive sodium channels, which appear to have resulted from exon duplication, E23c might have evolved from the conversion of an intronic sequence. Although a functional role for Na_v1.9b has yet to be established, intron-to-exon conversion may represent a mechanism for ion channels to acquire novel features.

Index Entries: Voltage-gated; ion channels; tetrodotoxin-resistant; alternative splicing; AT-AC introns; Na_v 1.9/NaN.

* Author to whom all correspondence and reprint requests should be addressed. E-mail: stephen.waxman@yale.edu

Introduction

Voltage-gated sodium channels are membrane proteins that are responsible for the initiation and propagation of action potentials in excitable cells. Sodium channels from rat brain are heterotrimers composed of the pore-forming α-subunit (260 kDa) and two smaller β-subunits *(1).* Ten distinct α-subunits have been cloned from rat tissues, and orthologs of some of them have been characterized in other vertebrates *(2).* All of the α-subunits share a common overall structure with four domains, each containing six transmembrane segments (*See* Fig. 1A). As a result of differences in their amino acid sequences, however, the different α-subunits display different voltage-dependence and kinetics and subcellular localization, and these can confer unique properties on various types of neurons *(3).*

The genes encoding sodium channel α-subunits are clustered at four chromosomal locations that may have arisen by two rounds of sequential duplication of a single-domain gene followed by gene duplication *(4)* (*see also* reviews in refs. *5* and *6*). It has also long been speculated that four-domain voltage-gated calcium channels have evolved from the single-domain potassium channel, and that voltage-gated sodium channels later evolved from the four-domain calcium channels by acquiring the new selectivity filter *(7).* However, a new picture is now emerging after the discovery of a single-domain voltage-gated sodium channel, although with a calcium channel-like pore region, in bacteria *(8).*

The exon/intron boundaries of several mammalian sodium channel genes have been determined *(9–15).* Although the majority of the introns belong to the prevalent U2-dependent, GT/AG class, introns of the U12-dependent AT/AC class are also represented at homologous positions *(9,15–17).* Minor class introns of the AT/AC type are detected in the genomic database at exceedingly low frequencies of 0.05% *(18,19).* The voltage-gated sodium channel family is unusual in that it is characterized by the conservation of multiple minor class introns among the genes that have been studied to date *(9–11,13–14,20–21,* and this review). The conservation of the minor class introns suggests the presence of these introns in the ancestral progenitor prior to the proposed duplication events that resulted in the generation of the four gene clusters in vertebrate genomes *(5).*

The minor class introns interrupt the coding sequence of voltage-gated sodium channels extending from jellyfish to mammals *(17,22).* It is remarkable, however, that the genes of the *para*-like voltage-gated sodium channels of insects that have been investigated to date lack minor class introns *(23).* The insect *para*-like sodium channel may have evolved from a different progenitor channel. Alternatively, the insect gene may be under selective pressure to convert its introns to the major class. It is intriguing that a few *Drosophila* genes contain minor class introns *(17),* suggesting that the pressure to convert the minor class introns of the voltage-gated sodium channel gene may not be universal.

The large number of exons comprising the voltage-gated sodium channel gene may provide a basis for the generation of a large number of isoforms by alternative splicing *(24).* Indeed, utilization of alternative exons "a" and "1" in the *para* sodium channel of *Drosophila* is associated with an increased channel density, possibly due to the presence of cAMP-dependent protein kinase (PKA) phosphorylation sites *(25).* An alternative transcript of $Na_v1.6$ (rPN4a/NaCh6/*Scn8a*) in rat tissues has an additional 11 amino acids in the cytoplasmic loop connecting domains I and II, and displays faster inactivation and recovery from inactivation kinetics compared to the shorter version when expressed in Xenopus oocytes *(26).* Developmentally-regulated and mutually exclusive alternative splicing of exon 5 (E5A and E5N) in domain I of several genes encoding TTX-S sodium channels results in a change of an asparagine residue in E5N to an aspartic acid residue in E5A *(27–30).* This change, however, has failed to produce a detectable effect on the properties of the channels when expressed in *Xenopus* oocytes *(31).* Developmentally regulated alternative splicing

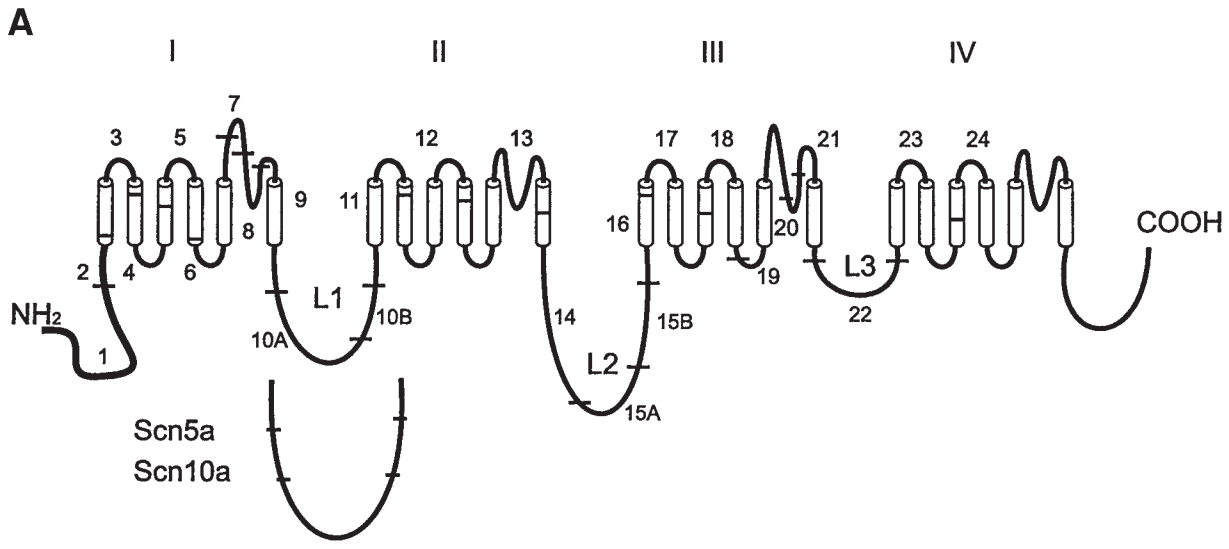

B

```
R    CTCTGTACCAGGAAGACAGgtaagcctt                    gtttctgggccaagGGTGAAGATG
Hu S GCTCAAGCCAGGAATCTCGgtaaggacc                    gtctctgtcctgagGGTGAAGATG
Hu L GCTCAAGCCAGGAATCTCGgtaaggacc   ccgcctcttgccagGTCCTCCAGGA//GGTGAAGATG
M    CTCCCTAGCAGGAAGACAGgtaagccat   tttctgccacacagTGTCTGAGCCAAGGGTGAAGATG
```

Fig. 1. Exon/intron map of *SCN11A*. **(A)** Exon/intron map of human *SCN11A* superimposed on the secondary structure of the channel. Sodium channel α-subunit consists of four domains (I–IV) that are linked with three intracellular loops (L1–L3). Each domain contains six transmembrane segments (S1–S6) that are connected by short linkers. The extracellular linkers joining S5 and S6 of each domain contain residues that line the pore, and form part of the selectivity filter of the channel. L1 is encoded by two exons in *SCN11A* whereas it is encoded by three exons in the case of *SCN5A* and *SCN8A*. **(B)** Exon/intron boundaries in the genomic segment of human, rat, and mouse *SCN11A* encoding 5′UTR sequences. The sequences of the terminal end of Na_v 1.9 cDNAs (capital letters), and the corresponding intron termini (lower case) from human, rat, and mouse are aligned. The arrow indicates the position of the 5′ splice site. The short (H_S) and long (H_L) forms of the 5′UTR of human Na_v 1.9 result from the utilization of the distal and proximal 3′ splice sites of this intron respectively. The slash marks (//) in the long version (H_L) of Na_v 1.9 represent nucleotide sequence not shown in this figure. The extra 13 nucleotides in the 5′ UTR of mouse Na_v 1.9 causes the apparent shift in the intron position compared to rat and human genes.

of exon 18 (E18A and E18 N), which is the domain III analog of E5, also occurs in mouse, human and fish $Na_v1.6$ *(30).* Unlike the highly conserved length and nucleotide sequence of the exon 5A/N pair, E18A and E18N vary significantly in length and sequence, and more importantly, E18N introduces a stop codon that results in a two-domain protein that has not been shown to assemble into a functional sodium channel *(30).*

Dib-Hajj et al. *(32)* recently identified the tetrodotoxin-resistant (TTX-R) sodium channel $Na_v1.9$ (NaN) encoded by the gene *SCN11A*. Mouse and human orthologs of this channel have also been identified *(9,33).* It is notable though that $Na_v1.9$ from mouse and rat is only 72% similar to that from human *(33).* In contrast, human and rat $Na_v1.5$ (SkM2) and $Na_v1.8$ (SNS), the two other TTX-R channels, are 82% and 93% similar, respectively. The physiology *(33–35)* and cell biology *(36–39)* of $Na_v1.9$ have been extensively studied. The channel is selectively expressed in functionally identified nociceptive primary sensory neurons of rat dorsal root ganglia (DRG) *(40).*

The gene structure of mouse *Scn11a*, and the chromosomal localization of both the human and mouse genes, have already been determined *(9). SCN11A* maps to chromosome 3 and to the syntenic locus on chromosome 9 of the mouse, in proximity to the two other TTX-R sodium channel genes *SCN5A* and *SCN10A (9),* which encode $Na_v1.5$ and $Na_v1.8$, respectively. The three genes encoding the TTX-R sodium channels are notable in lacking alternative exons 5 and 18. Trans-splicing, however, causes the duplication of exons 12–14 of $Na_v1.8$, but the channel is not functional in heterologous expression assays *(41),* and exon skipping yields functional $Na_v1.5$ channels with a shorter loop 2, linking domains 2 and 3 of the channel *(42,43).* The authors describe in this article the gene structure of human *SCN11A*, which is composed of at least 27 exons whose positions are conserved between mouse and human, and the origin of an alternative transcript $Na_v1.9b$. It is proposed that the alternative exon (E23c) arose by intron-to-exon conversion, and the potential implications of this mode of exon evolution for the development of novel features in other sodium channels is discussed below.

Identification of Exon/Intron Boundaries of *SCN11A*

The cDNA of human $Na_v1.9a$ *(33)* is encoded by 27 exons (*see* Table 2 and 3). The intron boundaries (Fig. 1A and Table 1) of human *SCN11A* interrupting the coding portion of the cDNA perfectly match those of the mouse gene *(9).* The sequence encoding the 5′UTR is interrupted by an intron (*see* Fig.1B), which utilizes alternative 3′ acceptor splice sites (GenBank Accession Number AF399967). The utilization of the proximal and distal 3′ splice sites, respectively, results in a 5′ UTR that is 239 nucleotides longer when the proximal site is used (Fig. 1B, and GenBank Accession Number AF399968). A partial sequence of the 5′ UTR that results from utilizing the proximal 3′ splice site has been reported *(44).*

PCR amplification, using primers 1–4 designed to amplify the 5′ end of rat and mouse $Na_v1.9a$ including the 5′ UTR (*see* Table 2), amplifies the expected product (256 bp in rat and 253 bp in mouse) from cDNA templates and a much larger product (about 5 kbp) from genomic templates. Sequencing the ends of the amplicons demonstrates the presence of an intron. The 3′ splice site of the intron in the mouse gene is shifted in the 5′ direction compared to that of the rat and the distal site in the human genes (Fig.1B). Inspection of the additional 13 nucleotides in the mouse $Na_v1.9$ 5′ UTR show that it has 11/13 and 8/13 matches to the 3′ terminal sequence of the introns interrupting the 5′ UTR of rat and human genes respectively; this sequence is part of the long 5′ UTR of the human gene (Fig. 1B). This may represent a case of activation of an upstream 3′ acceptor dinucleotide in the mouse intron, compared to the rat and human cognates, because introns are likely to utilize the first AG downstream of the branch site as the preferable 3′ splice site *(45–47).* There are no additional AG dinucleotides in the rat and human introns at the location corresponding to that of the mouse intron.

Except for introns 2 and 21 of *SCN11A* (Table 1) and its mouse ortholog *(9),* the intron termini match those predicted for the GT/AG major class of eukaryotic introns that are spliced by the U2-dependent splicesome *(16,48–51).* The termini of intron 2, ATATCC/CAC, and the consensus branch site, CCTTAATGG, are

Table 1
Exon-Intron Boundaries of Human *SCN11A*

	bp			bp			
U*	?	*ccaggaatctcg*	gtaaggacc	3019	acttgttc**ctgaa**ctcaacttcccgcctcttgccag	*gtcctccaggaatg*	1a
U*	?	*ccaggaatctcg*	gtaaggacc	3258	cctttc**tgag**gatctgtggcttgtctctgtcctgag	*ggtgaag* ATG GAT M D	1b
1	**	AAT CAT AAG N H K	gtacttcatt	3200	tgtgtgttttcttgtattgttttttttgttttgcag	ACA TTT ATG GTG T F M V	2
2	119	GTC CAT TC V H S	atatcctttc	1276	tcctgcaacatatctg**ccttaat**ggatgctggccac	A TTG TTC AGC L F S	3
3	102	ATT GCA GA I A E	gtaagtattt	5500	#	G TGT GTC TTC C V F	4
4	129	GGA ATA GC G I A	gtaagaatat	1300	agcaagcccatgccttccctgtgctttgtcttgtag	G ATT GTG TCA I V S	5
5	95	GTT TCA C V S	gtaagtcact	3800	ggatgggcttctccccaagcctgtcctctttctcag	GT CTG AAG GTC R L K V	6
6	180	GCT TAT G A Y	gtaaataccc	1100	tttaaaat**ctgaa**tttatgacttttttcctctctcag	AC CAT TGC TTT D H C F	7
7	67	GGT AAC AG G N S	gtaagaggtt	10000	tacataa**ttatt**tctctgtttgtttccaatatctag	T GCC TGT TCC A C S	8
8	142	TAT CAA CAG Y Q Q	gttatctatt	871	ggtttgatattcaagaacatgctctgtcctttgcag	ACC CTG CGT ACT T L R T	9
9	198	GAA AAG GAG E K E	gtagggacat	870	taatctgttctt**taat**tgcttttgttcaatttgaag	GCT CTG GTT GCC A L V A	10A
10A	174	CAA AAA AAG Q K K	gtaagtcttt	2800	ctgtctttagaaggtgccctatgccttctcttacag	CCA CAG CTC CTA P Q L L	10B
10B	130	ATG AAG G M K	gtaagttcca	1087	ag**ctaac**tcctcaacctctcgctcattctcctccag	AA CAA GAA AAA E Q E K	11
11	239	GGG AAT TTG G N L	gtaacattac	3600	agcttccttct**ctcat**tcttctttgtcccactctag	GTT TTC ACT AGC V F T S	12
12	180	TTC AGA GTG F R V	gtaaggcact	3000	ttttcttccatttttgtttgttgtctttttctacag	CTC AGG GTC TTC L R V F	13
13	381	AAA CTT GTG K L V	gtatgtgtct	2200	actttcctttcttcttgctacccaccccattcccag	GTG CTC AAC CTC V L N L	14
14	432	GAA CAA CAG E Q Q	gtatgaaggt	7000	aggaata**ttaat**tctattctgggctctctgtgttag	GCC TAT GAG CTC A Y E L	15A
15A	114	CCC CGA AAG P R K	gtaattttcc	722	taaaaggcacccccttcgttttgtt**ctgat**gtgcag	AAG TCT GAT GTT K S D V	15B
15B	115	CCC AAA G P K	gtaagtggca	2000	gaca**ctaat**gatagtgctaccattaattcctttcag	GC TTT GGT TGC G F G C	16
16	155	GGG GCA CTG G A L	gtaaatcatc	2800	t**tcaac**ctggcctatggctatgctttttcatttcag	ATA TTT GAA GAT I F E D	17
17	174	ATT GTG ATT I V I	gtaagtttac	8000	gtcaggtacattatctgtggcctctcttcccatcag	GTC TCT GTG ACC V S V T	18
18	102	GGA ATG AAG G M K	gtacattctg	484	atctgttatggttttctttgcttttgtttccataag	GTG GTG GTC AAT V V V N	19
19	264	CTG CAA GTG L Q V	gtaagtacag	700	atttgtattattcatgtttttctgcttttgttgcag	GCA ACA TTT AAG A T F K	20
20	54	TCC ACA GAG S T E	gtgagtcagt	2700	attgtttttttctc**ttat**taaaaaaatttctaacag	AAA GAA CAA CAG K E Q Q	21
21	138	CAG AAA AAG Q K K	ataagtatct	3700	tgttaaaggtaattagct**ctt**atcttctccatatac	TTA GGT GGC CAA L G G Q	22
22	105	CGG CCT CTG R P L	gtgagagca	>12000	cattcaaaatgatt**taat**tttcttttttttctcag	AAC AAA TGT CAA N K C Q	23
23	271	ATT GTT A I V	gtaagtaaaa	3000	ttctggaaa**cttat**ttacttttctccttctcctgag	GT ACA ATG ATT S T M I	24
24	1049	TGT GAC TGA C D *	3' UTR				

* Exon U in 5′UTR has been sequenced only at its 3′ end. It is followed by an intron of either 3019 bps or 3258 bps, depending on which of the two alternate 3′ splice sites are utilized.

** Exon 1 is either 513 bps or 274 bps, depending on which 3′ splice site in the upstream intron has been utilized (accession number AF399967).

The position of intron 3 was determined from its 5′ end; repeated sequencing from the 3′ end was unsuccessful.

Putative branch sites for U2- and U12-dependent introns are shown in boldface type. 5′ UTR is shown in italics.

Table 2
Primers for Na_v 1.9 Amplification

No.	Sequence	Species	Pos. in Na_v 1.9
1	GGAGCCATACGGTGCCCTGATC	Rat	4–25
2	GAATGTCACCATAAAGCTTAGG	Rat	259–238
3	CTGAGCCTCCCTAGCAGGAAGACAG	Mouse	8–32
4	GAACGTCGCCATAGAGCTTAGG	Mouse	260–239
5	ACGC**CTTAAG**GGTGCCCTGATCCTCTGTACCAGG[a]	Rat	14–37
6	*ATAAGAAT***GCGGCCGC**CAACCTGTCACCTCGTTCAGCC[b]	Rat	5477–5453
7	AACAAATGTCAAGCCTTTGTGTT	Rat	4048–4070
8	GGCGGGAAAGAAATGTCACTGTC	Rat	4364–4342
9	GTCACAAGCCAGGTCTTTGACG	Mouse	4082–4103
10	GTTGAAGTTCTCTAGAATCACAGCTATGT	Mouse	4816–4788
11	CTGAATCATACAACCAACCCAAAGC	Human	4184–4208
12	GACAATTCTGAAGAGCGTCGGAG	Human	4425–4403
13	TCTCGCCCTGCTGCAAGTGGC	Rat	3732–3752
14	TAATGATAGAAAGAACCACGA	Rat	4318–4298
15	CCTGAGGACCCGCTGAGGTCT	Rat	E23c

[a] Forward primer was designed to include a 5′ terminal GC clamp, a unique Afl II restriction enzyme recognition site (bold type) and 24 of 5′ untranslated nucleotides, 13 nucleotides upstream of the translation initiation codon ATG.

[b] Reverse primer was designed to include a terminal spacer (italic) a unique Not I restriction enzyme recognition site (bold type) and 3′ untranslated sequence.

excellent matches to the respective elements of the AT–AC minor class of eukaryotic pre-mRNA introns that are removed by the U12-dependent spliceosome *(16,49–51).* The termini of intron 21, ATAAG/TAC, are an excellent match to the respective termini of the rare AT–AC minor class of introns that are removed by the U2-dependent spliceosome *(16,49).*

Human Na_v1.9 is significantly less conserved among the three mammalian species *(33)* compared to other channels *(13,14).* The exon/intron boundaries of human *SCN11A*, however, are conserved compared to those of the mouse gene *(9)*, even in the regions encoding the less conserved intracellular and extracellular loops. Thus, Na_v1.9 is the same channel in the three species and the human sequence does not represent a new gene as previously suggested *(44).*

The three genes *SCN5A*, *SCN10A* and *SCN11A* share a common similar gene structure. The 5′UTR of *SCN11A* and *SCN5A* are interrupted by an intron, while the genomic organization of *SCN10A* encoding the 5′UTR is yet to be determined. The exon/intron boundaries in the regions encoding the channel polypeptide are conserved except for intracellular loops 1 and 2, and some of the extracellular linkers (*see* Fig.2). The presence of alternative exons in the genomic segments containing the L1 and L2 exons cannot be ruled out because the full sequence of these regions has yet to be reported. Loop 1 of *SCN11A* is one exon short compared to *SCN5A* and *SCN10A* (Fig. 2). It is notable that loop 2 of the three genes is composed of the same number of exons but its sequence is the most divergent of all regions of the channel *(32).* The divergence of loop 2 sequence in Na_v1.9 compared to Na_v1.5 and Na_v1.8 may reflect interactions with different cytosolic protein partners.

Table 3
Human Exon-Specific Primers

Exon	Forward	Intron	Reverse	Exon
5′	ATCTGCTCAAGCCAGGAATCTCG	5′	GGTACTTCTCCTGTCTGGTCTTTAG	1
1	GGTGAAGATGGATGACAGATGCT	1	GCATGCTTGGCACTGAAGCGGT	2
2	CTACCGCTTCAGTGCCAAGCATG	2	rATTCGCCATGAACATACAGTTGAT	3
3	ATCAACTGCGTGTTCATGGCTAC	3	ACTCATCCAGAATGAAACCTCTTGC	4
4	gGACCCRTGGAACTGGCTGGA	4	CACGGAAGGTACGCAGGGGCAAT	5
5	TTGCCCCTGCGTACCTTCCGTGTG	5	CAGTCCCTCGAGATGCATTTCAGG	6
6	GGCCTTGCTACGCTCTGTGAA	6	CACATTTTGAATTCAGGTGA	7
7	CACCTGAATTCAAAATGTGTGGC	7	gAAGAAGGGACCAGCCAAAGTTGTC	8
8	GCCTGTTCCATACAATATGAATG	8	TTCTTGTTCTGCTCCTCATATGC	9
9	GGCATATGAGGAGCAGAACAAGAAT	9	TTTGGGGTAAAATATGATGTTTCAAG	10A
10A	GAGTCTGGGAAAGACCAGCCTCC	10A	CTCCATGCTCATCAAAGTGGTCCA	10B
10B	CCAAACGACTGTCCCAGAATCTATC	10B	TGGTGATGGCCAGCTCAGTAAAC	11
11	CTGAGCTGGCCATCACCATCTG	11	GCCTCGGCGAAAGTAGTGGTAGG	12
12	CCTACCACTACTTTCGCCGAGG	12	GTGCCGTAAACATGAGACTGTCG	13
13	CTCAGTAGTTGGCATGCAGC	13	TTCATCTCCATGACCAGGGGAATG	14
14	ATTCCCCTGGTCATGGAGATGAA	14	ATCCTGTATGGTCAGATGAGGC	15A
15A	CGAGCCAGAGAGTTCAAAGTGTGG	15A	AACCATCTCAGGTAACCATCCAAAGC	15B
15B	ATCAGAATGTAGCACCATTGATC	15B	mCAGTGCTCCGCTGCTCAGCAG	16
16	CCTGGGTCATTTGGTGGAACCTG	16	GTCAGTACAATTTAGTAATTCTTGG	17
17	GTCAGTACAATTTAGTAATTCTTGG	17	TAGAGTCCGGAAGGACTTCAATT	18
18	mCTTGAAGTCCTTCCGGAATCTG	18	mATGAGGCAGACCAGCAAGACATTG	19
19	mGTCTTGCTGGTCTGCCTCATTTTC	19	GTTCTTTCTCTGTGGAATCAACAGCT	20
20	ACATTTAAGGGCTGGATGGATA	20	TACGAAGTAAATGTAACCGAGTGA	21
21	CTCGGTTACATTTACTTCGTAGT	21	GAGGCCGTGGAATGGGTTTTTGAG	22
22	TTAGGATCCAAAAAACCTCAAAAACCCAT	22	GGAAAGAAGCACGACCACACAGTC	23
23	CTGAATCATACAACCAACCCAAAGC	23	GACAATTCTGAAGAGCGTCGGAG	24
24	CTCCGACGCTCTTCAGAATTGTC	24	GCTATGAGGTAGGCGTGGAGGTG	

r denotes primer for rat $Na_v1.9$ sequence.

m denotes primer for mouse $Na_v1.9$ sequence.

g denotes primer for multiple Na channel sequences.

Isolation of an Alternative $Na_v1.9$ cDNA from Rat Tissues

Another $Na_v1.9$ transcript ($Na_v1.9b$) has been identified from rat DRG, which contains an open reading frame (ORF) of 1472 amino acid (a.a.) residues, compared to the expected ORF of 1765 a.a. of $Na_v1.9a$. The polypeptide sequence matches the published $rNa_v1.9a$ *(32)* through position 1378 of the amino acid sequence. The $rNa_v1.9b$ insert, however, contains a segment of novel amino acid sequence beginning at residue 1379. The nucleotide sequence 4187–4318 (132 bp) which encodes amino acid residues 1379–1423 (44 a.a.) in $rNa_v1.9a$ was replaced by a novel sequence (143 bp) that encodes 48 a.a. in $rNa_v1.9b$. The replaced amino acids make up transmembrane segment 2 (S2) and most of S3 of domain IV (DIV). The new sequence does not reconstitute the predicted transmembrane secondary structure of the protein. Furthermore, the new cDNA sequence introduces a +2 reading frame-shift that will terminate the mRNA

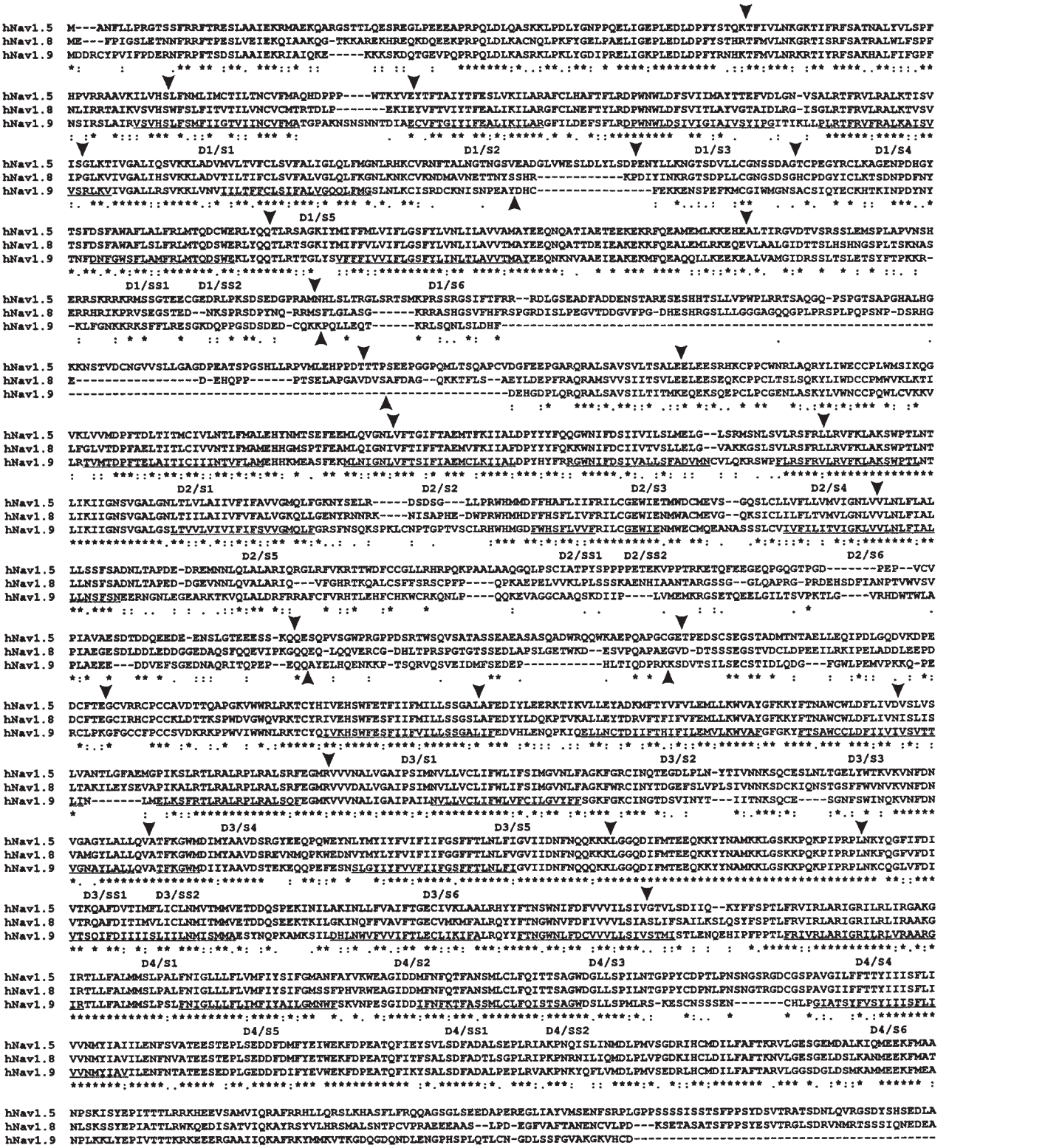
hNav1.5
hNav1.8
hNav1.9
D1/S1
D1/S2
D1/S3
D1/S4
D1/S5
D1/SS1
D1/SS2
D1/S6
D2/S1
D2/S2
D2/S3
D2/S4
D2/S5
D2/SS1
D2/SS2
D2/S6
D3/S1
D3/S2
D3/S3
D3/S4
D3/S5
D3/SS1
D3/SS2
D3/S6
D4/S1
D4/S2
D4/S3
D4/S4
D4/S5
D4/SS1
D4/SS2
D4/S6

Fig. 2. Alignment of the human TTX-R sodium channel sequences for Na_v 1.5, Na_v 1.8 and Na_v 1.9. The Clustal W algorithm is used to align the three polypeptides. The predicted transmembrane segments are underlined. The position of the exon/intron boundaries is superimposed on the amino acid sequence and is identified by an arrowhead. *SCN5A* and *SCN11A* have an additional intron interrupting the 5'UTR sequence. The respective region from *SCN10A* has yet to be analyzed. (*) represents identical amino acid residues in the three channels; (:) represent conservative substitutions; (–) represent deletions.

translation after another 46 a.a. Thus an alternative truncated protein may be produced that lacks transmembrane segments S2–S6 of DIV, and possesses a novel C-terminus.

In the genomic structure, amino acid residues 1379–1423 of $rNa_v1.9$ are encoded by the second half of exon 23 (E23). Mouse and rat E23 are each 271 bp long (*9*, and this review). The 5' half of E23 (1–139 bp which corresponds to nucleotides 4048–4186 of $rNa_v1.9a$) are conserved in $rNa_v1.9b$, and are designated here as E23a (*see* Fig.3). The 3' half of E23 (132 bp; corresponds to nucleotides 4187–4318 of rat $Na_v1.9a$), which encodes the 44 a.a. that were replaced in $rNa_v1.9b$, is designated here as E23b (Fig. 3). Thus, the novel sequence (143 bp) is designated E23c (Fig. 3; GenBank Accession Number 399965).

PCR amplification using a forward and reverse primer pair in E23a and E23b, respectively, and cDNA and genomic templates produced products of identical size (Dib-Hajj, S. D., Tyrrell, L., and Waxman S. G., unpublished), which confirms the absence of an intron interrupting the E23a and E23b coding sequences. Comparison of cDNA and genomic sequence, however, reveals the source of the new sequence in $rNa_v1.9b$. E23c is located 570 bp upstream from the 3' end of intron 23 (I23) (*see* Fig.4). The hexanucleotide start of E23b (corresponding to nucleotide 4187–4192 of $rNa_v1.9a$ sequence) matches the 5' splice site signal (ATATCC) of a U12-dependent AT–AC minor class intron (Figs. 3 and 4). The 23 nucleotides in the genomic sequence of I23, immediately upstream of E23c, contain the sequence CCTTAACT and the 3'terminal dinucleotide AC (Fig. 4), which represent the branch point and 3' splice site consensus signals, respectively, for the U12-dependent AT-

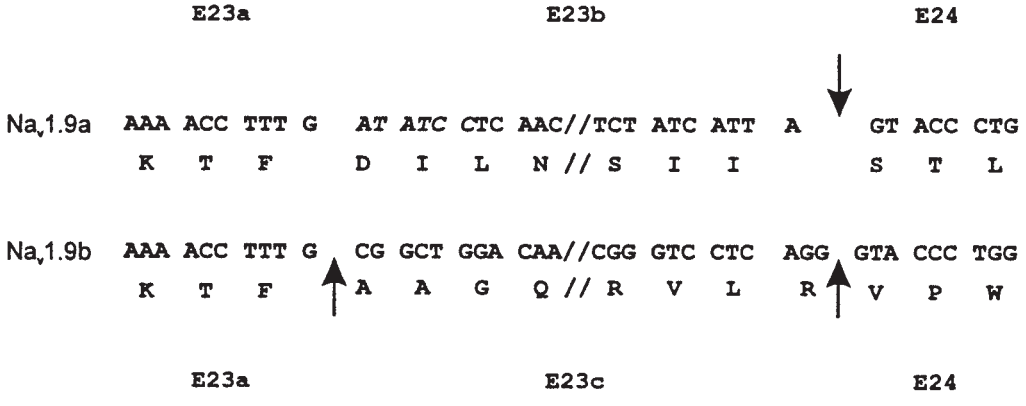

Fig. 3. Partial sequence of E23 in Na_v 1.9a and Na_v 1.9b. A portion of E23 from the two splice variants around the site of $I23alt_{AT\text{-}AC}$ are aligned to show the location of the intron separating E23a and E23c, and the E23/E24 junction. The 5' splice site of $I23alt_{AT\text{-}AC}$ defining the start of E23b is shown in italic type. The +2 frameshift that is introduced by E23c is shown at the juncture of E23c and E24. The slash marks represent sequences not shown in this figure.

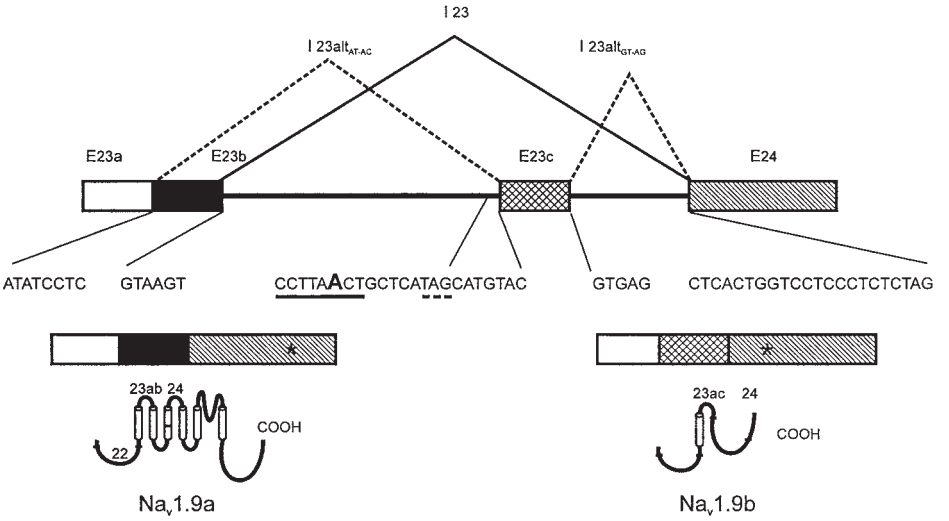

Fig. 4. Schematic diagram of rat *Scn11a* gene structure in the exon 22–24 region. Exon 23 (E23) of Na_v 1.9a is 271 nucleotides long. Nucleotides 1–139 are represented here as E23a (empty box). The sequence beginning at nucleotide 140 is the 5′ splice site (ATATCC) of a minor class U12-dependent AT-AC intron (I23alt$_{AT-AC}$). The remainder 132 nucleotides of E23 are represented here as E23b (filled box) are removed as part of splicing of this AT-AC intron. An alternative exon E23c (cross-hatched box) that is 143 bp long is used to replace E23b. Exon 23c is then followed by a U2-dependent GT-AG intron (I23alt$_{GT-AG}$) that is removed to splice E23c to E24 (hatched box). The consensus sequence for the branch site of I23alt$_{AT-AC}$ intron is underlined and the putative branch point adenosine nucleotide (A) is in bold face. The sequence TAG (underlined with a dashed line) is used as an alternative 3′ splice site that extends E23c by 7 nucleotides. The predicted secondary structures of the polypeptides encoded by exons 22–24 of Na_v 1.9a and Na_v 1.9b are shown below the schematic of the ligated exons. The cross-lines indicate the respective splicing patterns.

AC introns (I23alt$_{AT-AC}$) (Fig.4). Thus the sequence corresponding to E23b is removed during splicing of I23alt$_{AT-AC}$ (Fig. 4). The genomic sequence separating E23c and E24 show the hallmarks of a U2-dependent GT–AG intron (I23alt$_{GT-AG}$) that is removed to splice E23c to E24.

Expression of E23c in Rat DRG and Trigeminal Ganglia During Development

Na_v1.9b transcripts are present at low levels in rat DRG and trigeminal ganglia, and their amplification by nested RT–PCR is occasionally not detected, as seen in Figure 5. A minor 289 bp product with an additional 7 nucleotides at the 5′ end of E23c has also been detected. The additional 7 nucleotides are the result of utilizing a AG 3′ splice acceptor site of the I23alt$_{AT-AC}$ intron (Fig. 4). The additional 7 nucleotides to this E23c correct the reading frame-shift but introduce a stop codon 12 a.a. later. Furthermore, splicing of E23ac appears to be uniform across different developmental stages (*see* Fig. 6). DRG and trigeminal ganglia templates from E17, P0, P7, and P21 developmental stages contain comparable levels of Na_v1.9b transcripts.

The low abundance of the Na_v1.9b transcripts compared to Na_v1.9a is probably due to the dual function of E23b as an exon and the 5′ end of an intron. Intron I23alt$_{AT-AC}$ is poorly spliced, both in native neuronal tissues and in HEK293 cell line suggesting that the low level of splicing is an intrinsic property of this intron

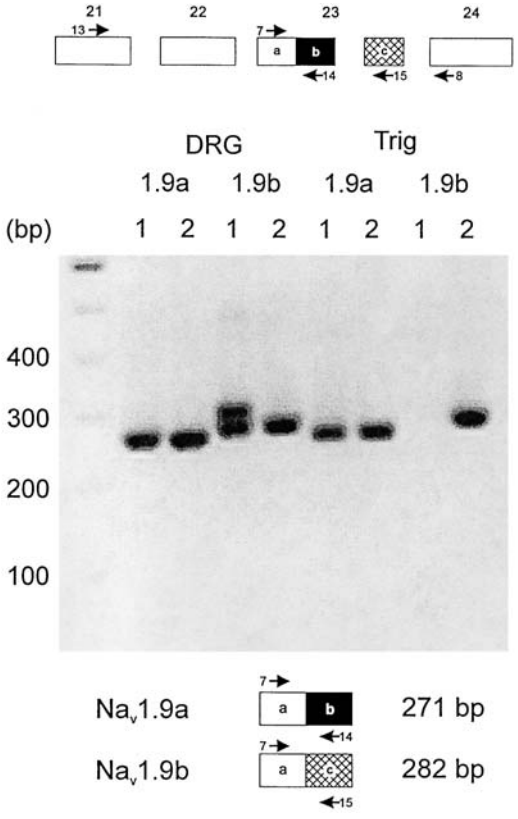

Fig. 5. RT-PCR amplification of E23ab and E23ac of Na$_v$ 1.9 from DRG and trigeminal ganglia. A schematic at the top of the gel shows the relative position of the different exons and the primary and secondary primers that were used in the RT-PCR assay. The primers are listed in Table 3. Two tissue samples (1 and 2) were independently analyzed for both DRG and trigeminal. The Na$_v$ 1.9a template amplifies a 271 bp fragment, while the Na$_v$ 1.9b template amplify a 282 bp and a 289 bp fragment. The 289 bp fragment results from the utilization of an AG, 7 nucleotides upstream of the AC splice site, as the terminal intron dinucleotide (*see* Fig. 4). The Na$_v$ 1.9b form is detected in both DRG and trigeminal cDNAs but its abundance is low; note that it is not detected in one of the trigeminal samples.

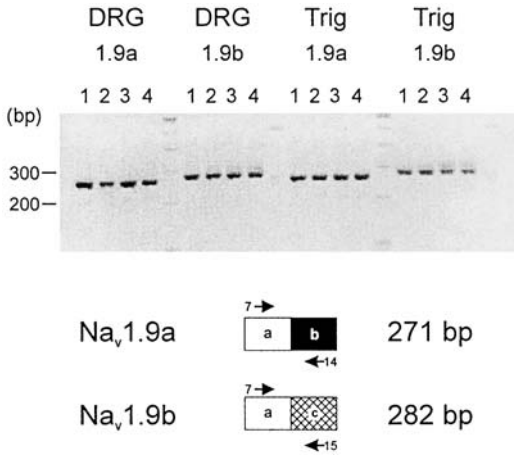

Fig. 6. Na$_v$ 1.9a and Na$_v$ 1.9b are present in rat DRG and trigeminal ganglia during development. Nested PCR for E23ab and E23ac reveals the presence of both transcripts at all stages of development from embryonic d 17–21 ds postnatal. Lanes 1–4 contain amplification products using templates from E17, P0, P7, and P21 respectively.

rather than the lack of a splicing factor. The competition between the I23$_{GT\text{-}AG}$ (E23b acting as an exon) and the I23alt$_{AT\text{-}AC}$ (E23b acting as the 5′ end of an intron) for the spliceosome machinery favors splicing of the major class GT/AG intron. The U12 snRNAs, which are required for the splicing of the AT/AC minor class introns, are 100× less abundant than their U2 counterparts that are used in the splicing of the GT/AG introns *(52)*. The splicing efficiency of the two other minor class introns that are present in *Scn11a (9)*, and that are common to the other voltage-gated sodium channel genes *(17)*, are not affected because they have no GT/AG major class intron competitors at their respective sites.

Sequence of E23c in Human and Mouse SCN11A

The sequence of exon 23 splice sites for rat, human, and mouse are compared in Figure 7. The nucleotide sequences of rat and mouse E23ab are 94% identical. Exon 23c is 143 bp long in the rat and 142 bp long in the mouse (GenBank Accession Number 399966) with an overall 88.8% identity at the nucleotide level. E23c is clearly defined in rat *Scn11a* by the 3′ splice site of the upstream intron I23alt$_{AT\text{-}AC}$ and the 5′ splice site of the downstream intron

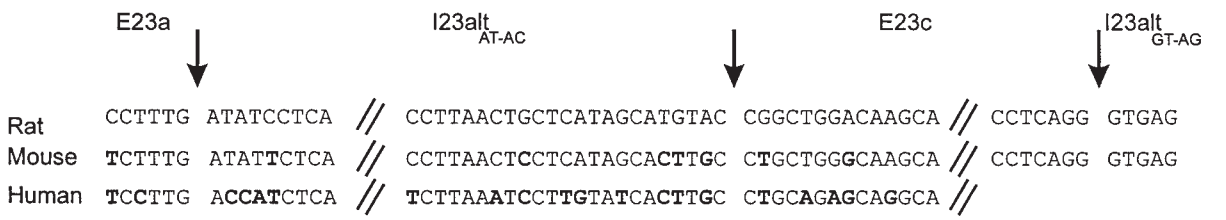

Fig. 7. Alignment of the genomic sequence around the region of E23a and E23c of *SCN11A* from rat, mouse, and human. The location of the 5′ and 3′ splice sites of $I23alt_{AT-AC}$, respectively, are shown by the first two arrows from left to right. The third arrow designates the 5′ splice site of $I23alt_{GT-AG}$. Nucleotide sequence in bold face type is different from that of the rat sequence. The slashes (//) indicate sequences not shown in the figure.

$I23alt_{GT-AG}$ (Figs. 4 and 7). Mouse *Scn11a* contains the CCTTAACT sequence, 23 bp upstream of E23c, which perfectly matches the recognition site for lariat formation. The 3′ splice site, however, is GC in the mouse gene compared to AC in the rat gene (Fig. 7). Both rat and mouse genomic sequences have the conserved GTGAG 5′ splice site signal of the U2-dependent intron $I23alt_{GT-AG}$ separating E23c and E24. The 5′ splice of $I23alt_{AT-AC}$ in mouse E23 has a single nucleotide substitution ATAT*T*C (C to T substitution, italic) compared to rat sequence (Fig. 7). An alternate $Na_v1.9b$ transcript in mouse DRG and trigeminal tissues has not been detected by RT–PCR despite the conservation of these splice-site signals. Moreover, splicing of mouse E23c has not been detected in HEK293 cells that are transfected with a genomic DNA clone containing exons E23ab, E23c, and E24 and the intervening introns (data not shown). The single nucleotide substitutions in the 5′ and 3′ splice sites of the mouse $I23alt_{AT-AC}$ separating E23a and E23c appear to be sufficient to prevent the splicing of this intron both in native tissues and in transfected HEK 293 cell line.

Human and rat E23ab are conserved in length (271 bp) and are 80% identical at the nucleotide level. Figure 7 shows that the two splice sites and branch site sequences of $I23alt_{AT-AC}$ in human *SCN11A* are divergent compared to the consensus sequences. The putative 5′ splice site ACCATC is only identifiable by alignment with the rat sequence, and the recognition sequence for lariat formation, TCTTAAAT, is also divergent compared to the consensus sequence. Finally, the 3′ splice site is GC instead of the consensus AC. Transcripts that contain the putative alternative E23c have not been detected by RT–PCR from human DRG.

The variant splicing signals in human and mouse $I23alt_{AT-AC}$ may render them unrecognizable by the spliceosome machinery, thus preventing the utilization of E23c. The substitution of the penultimate nucleotide "A" by "G" has been reported to prevent splicing of a model AT/AC intron both in vitro and in vivo *(53).* The 3′ splice site dinucleotide GC in mouse $I23alt_{AT-AC}$ thus could prevent splicing of this intron in mouse tissues and HEK 293 cells. Similarly, human $I23alt_{AT-AC}$ intron possesses divergent 5′ and 3′ splice-site signals that can prevent splicing of this intron and hence the lack of $Na_v1.9b$ in human DRG tissues. This finding provides a naturally occurring example of a variant 3′ splice site that confirms the data of Dietrich et al. *(53).*

Implications for *SCN11A* Gene Evolution

The presence of alternative transcripts that result in truncated proteins such as $Na_v1.9b$

may reflect an evolutionary mechanism for acquiring novel functions. This may be especially advantageous for sodium channels since fucntional channel expression at an appropriate level is critical for neuronal function. Ion channel derivatives with two or three domains may acquire novel functions, for example as a "fail-safe" mechanism to prevent expression of a functional $Na_v1.6$ channel in non-neuronal tissues *(30),* or as a dominant negative regulator of calcium channels *(54).* Although a function has not been attributed to $Na_v1.9b$, its presence may shed a new light on the evolution of the *SCN11A* gene.

Rat *Scn11a* has a novel feature not shared by the other voltage-gated sodium channels. Exon 23 is composed of two parts that are contributed by E23a and E23b, which doubles as the 5′ portion of a minor class AT/AC, U12-dependent intron. This genomic organization of E23ab and E23c may reflect the design of an ancestral gene of this lineage. If the E23ab and E23c organization reflects the architecture of a progenitor gene, then the lack of a recognizable $I23alt_{AT\text{-}AC}$ intron at a comparable position in other sodium channel genes suggests the loss of functional splicing signals prior to the gene duplication events that produced the cluster of the three TTX-R genes (located on chromosome 3 in humans, and chromosome 9 in mouse) and prior to the duplication events that produced the other three independent TTX-S sodium channel gene clusters.

The selective presence of E23c in *Scn11a,* however, could have resulted from the more recent conversion of an intron sequence into an exon, accompanied by the acquisition of the splicing signals to remove $I23alt_{AT\text{-}AC}$ and ligate E23a and E23c (Fig.4). An intron-to-exon conversion has been reported in the dystrophin gene, where a novel exon appears to have been established during the evolution of hominoids by the acquisition of the consensus signals for a GT/AG, U2-dependent splicing *(55).* Unlike exon duplication that accounts for the origin of exons 5A and 5N, where the alternative exons differ by only one or two amino acids *(27–30),* intron conversion does not require *a priori* that the new exon conserve the length or the reading frame of its replacement. E23c is longer by 11 bp than E23b and introduces a premature translation termination codon, which truncates domain 4. Another example of alternative exons that differ in length, and where one exon introduces a translation termination codon, has been described in Scn8a *(14).* Exon 18N (70 bp in human and 68 bp in mouse) is shorter than E18A (123 bp) and encodes 9 a.a. before the translation termination codon, which produces a polypeptide that is truncated at the end of transmembrane segment 3 in domain 3 *(14).*

Because E23c of *Scn11a* and E18N of *SCN8A* do not conserve the length or the coding potential of their alternate exons, the case for exon duplication to account for their origin is significantly weaker than the case for E5A and E5N. However, Meisler and colleagues argued for exon duplication to account for the origin of E18N of *SCN8A* because amino acid residues of E18N from human, mouse, and fish are conserved at multiple positions compared to E18A *(14).* It is well established that gene families, for example the family of voltage-gated sodium channels, evolve by gene duplication followed by mutations. Members of these families have been thought to acquire new properties by substituting amino acids at key positions, or by utilizing alternative exons that arise by exon duplication followed by sequence divergence. On the basis of these observations, the authors propose that an alternative model, intron-to-exon sequence conversion, may provide a mechanism for evolving new functions for members of gene families. The success of intron-to-exon conversion is dependent upon the occurrence of this event in genomic segments which encode polypeptide regions that tolerate sequence change, for example intracellular loops of the sodium channels, and the conservation of the ORF. The long evolutionary history of the sodium channel gene family, from jellyfish to human, suggest that both mechanisms for generating novel sequences may have contributed to the rich repertoire of

sodium-channel phenotypes that are present in excitable tissues.

Acknowledgments

We thank Dr. Miriam Meisler for helpful discussions. This work was supported in part by grants from the National Multiple Sclerosis Society and the Rehabilitation Research and Development Service and Medical Research Services, Department of Veterans Affairs, and by gifts from the Paralyzed Veterans of America and Eastern Paralyzed Veterans Association.

The nucleotide sequences reported in this paper have been submitted to GenBank (GenBank Accession Numbers: AF399965, AF399966, AF399967, AF399968).

References

1. Catterall W. A. (2000) From ionic currents to molecular mechanisms: the structure and function of voltage-gated sodium channels. *Neuron* **26,** 13–25.
2. Goldin A. L., Barchi R. L., Caldwell J. H., et al. (2000) Nomenclature of voltage-gated sodium channels. *Neuron* **28,** 365–368.
3. Waxman S. G. (2000) The neuron as a dynamic electrogenic machine: modulation of sodium-channel expression as a basis for functional plasticity in neurons. *Philos. Trans. R. Soc. Lond. B. Biol. Sci* **355,** 199–213.
4. Strong M., Chandy K. G., and Gutman G. A. (1993) Molecular evolution of voltage-sensitive ion channel genes: on the origins of electrical excitability. *Mol. Biol. Evol.* **10,** 221–242.
5. Plummer N. W., and Meisler M. H. (1999) Evolution and diversity of mammalian sodium channel genes. *Genomics* **57,** 323–331.
6. Anderson P. A. and Greenberg, R. M. (2001) Phylogeny of ion channels: clues to structure and function. *Comp. Biochem. Physiol. B. Biochem. Mol. Biol.* **129,** 17–28.
7. Hille B. (1991) *Ionic Channels of Excitable Membranes* (2nd Ed.), Sinauer Publ. Co., Sunderland, MA 01375.
8. Ren D., Navarro B., Xu H., Yue L., Shi Q., and Clapham D. E. (2001) A prokaryotic voltage-gated sodium channel. *Science* **294,** 2372–2375.
9. Dib-Hajj S. D., Tyrrell L., Escayg A., Wood P. M., Meisler M. H., and Waxman S. G. (1999) Coding sequence, genomic organization, and conserved chromosomal localization of the mouse gene Scn11a encoding the sodium channel NaN. *Genomics* **59,** 309–318
10. McClatchey A. I., Lin C. S., Wang J., Hoffman E. P., Rojas C., and Gusella J. F. (1992). The genomic structure of the human skeletal muscle sodium channel gene. *Hum. Mol. Genet.* **1,** 521–527.
11. George A. L., Jr., Iyer G. S., Kleinfield R., Kallen R. G., and Barchi R. L. (1993) Genomic organization of the human skeletal muscle sodium channel gene. *Genomics* **15,** 598–606.
12. Wang Q., Li Z., Shen J., and Keating M. T. (1996) Genomic organization of the human SCN5A gene encoding the cardiac sodium channel. *Genomics* **34,** 9–16.
13. Souslova V. A., Fox M., Wood J. N., and Akopian A. N. (1997) Cloning and characterization of a mouse sensory neuron tetrodotoxin-resistant voltage-gated sodium channel gene, Scn10a. *Genomics* **41,** 201–209.
14. Plummer N. W., Galt J., Jones J. M., Burgess D. L., Sprunger L. K., Kohrman D. C., and Meisler M. H. (1998) Exon organization, coding sequence, physical mapping, and polymorphic intragenic markers for the human neuronal sodium channel gene SCN8A. *Genomics* **54,** 287–296.
15. Kasai N., Fukushima K., Ueki Y., et al. (2001) Genomic structures of SCN2A and SCN3A—candidate genes for deafness at the DFNA16 locus. *Gene* **264,** 113–122.
16. Dietrich R. C., Incorvaia R., and Padgett R. A. (1997) Terminal intron dinucleotide sequences do not distinguish between U2- and U12-dependent introns. *Mol Cell* **1,** 151–160.
17. Wu Q. and Krainer A. R. (1999) AT-AC Pre-mRNA splicing mechanisms and conservation of minor introns in voltage-gated ion channel genes. *Mol. Cell Biol.* **19,** 3225–3236.
18. Burset M., Seledtsov I. A., and Solovyev V. V. (2000) Analysis of canonical and non-canonical splice sites in mammalian genomes. *Nucl. Acids Res.* **28,** 4364–4375.
19. Burset M., Seledtsov I. A., and Solovyev V. V. (2001) SpliceDB: database of canonical and non-canonical mammalian splice sites. *Nucl. Acids Res.* **29,** 255–259.
20. Kohrman D. C., Harris J. B., and Meisler M. H. (1996) Mutation detection in the med and medJ alleles of the sodium channel Scn8a. Unusual

splicing due to a minor class AT-AC intron. *J. Biol. Chem.* **271,** 17,576–17,581.
21. Wu Q. and Krainer A. R. (1997) Splicing of a divergent subclass of AT-AC introns requires the major spliceosomal SnRNAs. *RNA* **3,** 586–601.
22. Spafford J. D., Spencer A. N., and Gallin W. J. (1999) Genomic organization of a voltage-gated Na+ channel in a hydrozoan jellyfish: insights into the evolution of voltage-gated Na+ channel genes. *Receptors Channels* **6,** 493–506.
23. Park Y., Taylor M. F. J., and Feyereisen R. (1999) Voltage-gated sodium channel genes hscp and hDSC1 of Heliothis virescens F-genomic organization. *Insect Mol. Biol.* **8,** 161–170.
24. Thackeray J. R. and Ganetzky B. (1994) Developmentally regulated alternative splicing generates a complex array of Drosophila para sodium channel isoforms. *J. Neurosci.* **14,** 2569–2578.
25. O'Dowd D., Gee J. R., and Smith M. A. (1995) Sodium current density correlates with expression of specific alternatively spliced sodium channel mRNAs in single neurons. *J. Neurosci.* **15,** 4005–4012.
26. Dietrich P. S., McGivern J. G., Delgado S. G., Koch B. D., Eglen R. M., Hunter J. C., and Sangameswaran L. (1998) Functional analysis of a voltage-gated sodium channel and its splice variant from rat dorsal root ganglia. *J. Neurochem.* **70,** 2262–2272.
27. Sarao R., Gupta S. K., Auld V. J., and Dunn R. J. (1991) Developmentally regulated alternative RNA splicing of rat brain sodium channel mRNAs. *Nucl. Acid Res.* **19,** 5673–5679.
28. Gustafson T. A., Clevinger E. C., O'Neill T. J., Yarowsky P. J., and Kreuger B. K. (1993) Mutually exclusive exon splicing of type III brain sodium channel alpha subunit RNA generates develomentally regulated isoforms in rat brain. *J. Biol. Chem.* **268,** 18,648–18,653.
29. Belcher S. M., Zerillo C. A., Levenson R., Ritchie J. M., and Howe J. R. (1995) Cloning of a sodium channel alpha subunit from rabbit Schwann cells. *Proc. Natl. Acad. Sci. USA* **92,** 11,034–11,038.
30. Plummer N. W., McBurney M. W., and Meisler M. H. (1997) Alternative splicing of the sodium channel SCN8A predicts a truncated two-domain protein in fetal brain and non-neuronal cells. *J. Biol. Chem.* **272,** 24,008–24,015.
31. Auld V. J., Goldin A. L., Krafte D. S., Catterall W. A., Lester H. A., Davidson N., and Dunn R. J. (1990) A neutral amino acid change in segment IIS4 dramatically alters the gating properties of the voltage-dependent sodium channel. *Proc. Natl. Acad. Sci. USA* **87,** 323–327.
32. Dib-Hajj S. D., Tyrrell L., Black J. A., and Waxman S. G. (1998) NaN, a novel voltage-gated Na channel, is expressed preferentially in peripheral sensory neurons and down-regulated after axotomy. *Proc. Natl. Acad. Sci. USA* **95,** 8963–8968.
33. Dib-Hajj S. D., Tyrrell L., Cummins T. R., Black J. A., Wood P. M., and Waxman S. G. (1999) Two tetrodotoxin-resistant sodium channels in human dorsal root ganglion neurons. *FEBS Letters* **462,** 117–120.
34. Cummins T. R., Dib-Hajj S. D., Black J. A., Akopian A. N., Wood J. N., and Waxman S. G. (1999) A novel persistent tetrodotoxin-resistant sodium current In SNS-null and wild-type small primary sensory neurons. *J. Neurosci.* **19,** RC43.
35. Herzog R. I., Cummins T. R., and Waxman S. G. (2001) Persistent TTX-resistant Na(+) current affects resting potential and response to depolarization in simulated spinal sensory neurons. *J. Neurophysiol.* **86,** 1351–1364.
36. Sleeper A. A., Cummins T. R., Dib-Hajj S. D., Hormuzdiar W., Tyrrell L., Waxman S. G., and Black J. A. (2000) Changes in expression of two tetrodotoxin-resistant sodium channels and their currents in dorsal root ganglion neurons after sciatic nerve injury but not rhizotomy. *J. Neurosci.* **20,** 7279–7289.
37. Liu Cj C., Dib-Hajj S. D., Black J. A., Greenwood J., Lian Z., and Waxman S. G. (2001) Direct interaction with contactin targets voltage-gated sodium channel Nav1.9/NaN to the cell membrane. *J. Biol. Chem.* **276,** 46,553–46,561.
38. Liu C., Dib-Hajj S. D., and Waxman S. G. (2001) Fibroblast growth factor homologous factor 1B binds to the C terminus of the tetrodotoxin-resistant sodium channel rNav1.9a (NaN). *J. Biol. Chem.* **276,** 18,925–18,933.
39. Tyrrell L., Renganathan M., Dib-Hajj S. D., and Waxman S. G. (2001)) Glycosylation alters steady-state inactivation of sodium channel Nav1.9/NaN in dorsal root ganglion neurons and is developmentally regulated. *J. Neurosci.* **21,** 9629–9637.
40. Lawson S. N., Black J. A., Dib-Hajj S. D., Waxman S. G., Cummins T. R., Djouhri L., and Fang X. (2001) Sensory and electrophysiological properties of DRG neurones with NaN-like immunoreactivity (NaN-LI) in rats. *Scociety for Neuroscince Abstract* 819.6.

41. Akopian A. N., Okuse K., Souslova V., England S., Ogata N., and Wood J. N. (1999) Trans-splicing of a voltage-gated sodium channel is regulated by nerve growth factor. *FEBS Letters* **445,** 177–182.
42. Gersdorff Korsgaard M. P., Christophersen P., Ahring P. K., and Olesen S. P. (2001) Identification of a novel voltage-gated Na+ channel rNa(v)1.5a in the rat hippocampal progenitor stem cell line HiB5. *Pflugers Arch.* **443,** 18–30.
43. Zimmer T., Bollensdorff C., Haufe V., Birch-Hirschfeld E., and Benndorf K. (2002) Mouse heart Na(+) channels: primary structure and function of two isoforms and alternatively spliced variants. *Am. J. Physiol. Heart Circ. Physiol.* **282(3),** H1007–1017.
44. Jeong S. Y., Goto J., Hashida H., Suzuki T., Ogata K., Masuda N., Hirai M., Isahara K., Uchiyama Y., and Kanazawa I. (2000) Identification of a novel human voltage-gated sodium channel alpha subunit gene, SCN12A. *Biochem. Biophys. Res. Commun.* **267,** 262–270.
45. Chen S., Anderson K., and Moore M. J. (2000) Evidence for a linear search in bimolecular 3′ splice site AG selection. *Proc. Natl. Acad. Sci. USA* **97,** 593–598.
46. Anderson K. and Moore M. J. (1997) Bimolecular exon ligation by the human spliceosome. *Science* **276,** 1712–1716.
47. Nelson K. K. and Green M. R. (1989) Mammalian U2 snRNP has a sequence-specific RNA-binding activity. *Genes Dev.* **3,** 1562–1571.
48. Senapathy P., Shapiro M. B., and Harris N. L. (1990) Splice junctions, branch point sites, and exons: sequence statistics, identification, and applications to genome project. *Meth. Enzymol.* **183,** 252–278.
49. Sharp P. A. and Burge, C. B. (1997) Classification of introns: U2-type or U12-type. *Cell* **91,** 875–879.
50. Tarn W. Y. and Steitz J. A. (1997). Pre-mRNA splicing: the discovery of a new spliceosome doubles the challenge. *TIBS* **22,** 132–137.
51. Mount S. M. (1996) AT-AC introns: an ATtACk on dogma. *Science* **271,** 1690–1692.
52. Montzka K. A. and Steitz J. A. (1988). Additional low-abundance human small nuclear ribonucleoproteins: U11, U12, etc. *Proc. Natl. Acad. Sci. USA* **85,** 8885–8889.
53. Dietrich R. C., Peris M. J., Seyboldt A. S., and Padgett R. A. (2001) Role of the 3′ splice site in U12-dependent intron splicing. *Mol. Cell Biol.* **21,** 1942–1952.
54. Raghib A., Bertaso F., Davies A., Page K. M., Meir A., Bogdanov Y., and Dolphin A. C. (2001) Dominant-negative synthesis suppression of voltage-gated calcium channel cav2.2 induced by truncated constructs. *J. Neurosci.* **21,** 8495–8504.
55. Dwi Pramono Z. A., Takeshima Y., Surono A., Ishida T., and Matsuo M. (2000) A novel cryptic exon in intron 2 of the human dystrophin gene evolved from an intron by acquiring consensus sequences for splicing at different stages of anthropoid evolution. *Biochem. Biophys. Res. Commun.* **267,** 321–328.